COBEM 2021 26th International Congress of Mechanical Engineering
November 22-26, 2021, Virtual Congress, Brazil

# COB-2021-1980
# THE INFLUENCE OF A NON-CONSTANT INERTIA IN TORSIONAL VIBRATION OF A RECIPROCATING COMPRESSOR

**Nícolas da Silva Dias**
**Aline Souza de Paula**
Universidade de Brasília, Campus Universitário Darcy Ribeiro, Faculdade de Tecnologia, Asa Norte, CEP 70.910-900, Brasília-DF
nicolassd29@gmail.com
alinedepaula@unb.br

***Abstract.*** *Torsional vibrations are usually present at some level in rotating machines, as in motors and reciprocating compressors. The majority of works in the literature consider simplified linear models in the dynamical analysis of these systems, which can lead to important errors. This work considers a simplified nonlinear reciprocating compressor shaft model with variable inertia of the rod-crank-piston mechanism. The model, which consists of a single cylinder compressor attached to an electric motor, is evaluated in order to analyze the influence of the variable inertia in the dynamical behavior. A parametric analysis is carried out and the results show that the nonlinearities due to non-constant inertia are evident in the torsional vibration response. When considering an additional harmonic excitation, the influence of the nonlinearities is even more important and complex responses can emerge depending on the geometric dimensions and forcing frequency and amplitude of harmonic excitation. The results show the importance of considering the nonlinearities due to the variable inertia of the mechanism.*

***Keywords:*** *nonlinearities, torsional vibration, reciprocating compressor, non-constant inertia*

## 1. INTRODUCTION

In all rotating machines, as in the case of reciprocating compressors, some level of torsional vibrations is usually present, either during startup, steady operation or in the shutdown of the equipment. Therefore, it is essential to analyze the torsion response of the system to ensure high reliability and long service machinery life (Wachel and Szenasi, 1993). In general, these vibrations are caused by the excessive forces and moments that varies cyclically with periodicity given by system rotation speed, and can lead to failures of mechanical components such as the crankshaft and bearings (Wachel *et al.*, 1994).

The mathematical models used in the literature to describe rotating machines with crankshaft can be linear and non-linear. The first group considers that the inertia of rod-crank-piston mechanism is constant. This assumption can lead to important errors depending on geometric dimensions of the equipment and operational conditions. Metallidis and Natsiavas (2003) and Huang *et al.* (2012) present a more representative model by considering that the mechanism inertia varies with the rotation, resulting in nonlinear equations of motion. Several studies have made contributions to investigate the influence of a non-constant inertia effects. Brusa *et al.* (1997) carried out an analysis of torsional vibration by comparing and showing the different in dynamical response of the classical linear model with constant inertia and a nonlinear model with variable inertia. Pasricha and Carnegie (1976, 1979) discussed about a phenomena called secondary resonance which appears in torsional vibrations of crankshafts of multi-cylinders diesel engines. In the present work, a nonlinear model of a reciprocating compressor shaft that considers variable inertia of rod-crank-piston mechanism is considered. Huang *et al.* (2012) consider the same system and a similar approach when modelling the system, however, simplifications in the equation of the variable inertia as well as in the governing equations are considered. Metallidis and Natsiavas (2003) also considers variable inertia, however, the dynamic analysis is performed only in the transient regime. In this paper, a simplified model of a reciprocating compressor with only one cylinder attached to an electric motor through a shaft is of concern. The dynamical analysis is carried out mainly in steady-state regime focusing on the influence of nonlinearities in torsional vibration.

## 2. PROBLEM DESCRIPTION

According to the physical model proposed by Metallidis and Natsiavas (2003), it is assumed that alternative machines are divided into two parts. The first is the compressor itself and the second represents the load. Figure 1 presents a simplified scheme that represents a single-cylinder reciprocating compressor.

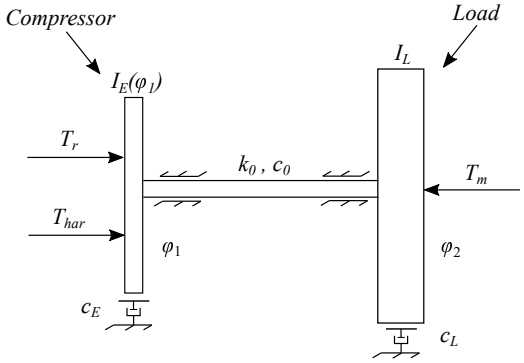


Figure 1: Equivalent model for a reciprocating compressor with a single cylinder.

As shown in Figure 1, the variable inertia of the cylinder is symbolized by $I_E(\varphi_1)$ which depends on the crank angle ($\varphi_1$). The load has constant inertia represented by $I_L$ which is related to transmission parameters such as its inertia and numerical transmission ratio (Metallidis and Natsiavas, 2003). Furthermore, the angular displacement of the load is represented by $\varphi_2$. The shaft that couples these parts has an equivalent torsional stiffness $k_0$ and viscous damping $c_0$. There is also a viscous damping associated with each part, $c_E$ and $c_L$. In addition, the external torques applied to the system are the resistive torque developed by the compression of the gas in the cylinder, $T_r$, the drive torque delivered by the electric motor, $T_m$, and an additional harmonic torque, $T_{har}$.

### 2.1 Derivation of equivalent inertia for a single cylinder

In the crank-rod-piston mechanism, shown in Figure 2, the crank rotates along the axis of rotation (crankshaft) transmitting movement and power to the connecting rod, which in turn triggers the piston to perform a movement alternative (Huang *et al.*, 2012). The crank length is described by $r$, $l_G$ is the distance from the end of the crank to the center of mass of the connecting rod, $l$ is the total length of the connecting rod, $F_p(\varphi_1)$ is the resultant force of the compression in the cylinder, besides that $\beta$ is the angle between the connecting rod and the axis $x$.

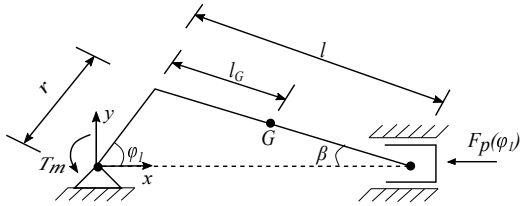


Figure 2: Crank-rod-piston mechanism.

The total kinetic energy of this mechanism is:

$$T_E = \frac{1}{2}\{I_c + m_1 r^2 + I_2\kappa^2(\varphi_1) + (m_2 + m_p)r^2 sen^2(\varphi_1)[1 + \kappa(\varphi_1)]^2\}\dot{\varphi_1}^2 \tag{1}$$

where $I_c$ is the moment of inertia of the crank, $I_G$ and $m_r$ are respectively the moment of inertia of the center of mass and the mass of the connecting rod. In addition, $m_p$ represents the piston mass and $\dot{x}_p$ is its velocity, $m_1$ is the mass of big end, $m_2$ is the mass of small end, and $I_2$ is an additional inertia from simplified double-mass system. Additionally, $\kappa(\varphi_1)$ and $\lambda$ are given by:

$$\kappa(\varphi_1) = \frac{\lambda cos(\varphi_1)}{\sqrt{1 - \lambda^2 sen^2(\varphi_1)}} \qquad\qquad \lambda = \frac{r}{l}. \tag{2}$$

Since the kinetic energy is given by $\frac{1}{2}I_E(\varphi_1)\dot{\varphi_1}^2$, the inertia of the mechanism is:

$$I_E(\varphi_1) = I_c + m_1 r^2 + I_2\kappa^2(\varphi_1) + (m_2 + m_p)r^2 sen^2(\varphi_1)[1 + \kappa(\varphi_1)]^2. \tag{3}$$

The equations of motion are obtained using the Lagrangian formulation:

$$\frac{d}{dt}\left(\frac{\partial T}{\partial \dot{\varphi}_i}\right) - \frac{\partial T}{\partial \varphi_i} + \frac{\partial U}{\partial \varphi_i} + \frac{\partial D}{\partial \dot{\varphi}_i} = Q_i, i = 1, 2 \tag{4}$$

where $T$ is the kinetic energy, $U$ is the potential energy, $D$ is the dissipative energy and $Q$ is the general torques.

So, after employing the Lagrange's equation (Eq. 4) to the 2 DOF system, the government equations are determined by following set of equations:

$$I_E(\varphi_1)\ddot{\varphi_1} + \frac{1}{2}\frac{dI_E(\varphi_1)}{d\varphi_1}\dot{\varphi_1}^2 + c_0(\dot{\varphi_1} - \dot{\varphi_2}) + c_E\dot{\varphi_1} + k_0(\varphi_1 - \varphi_2) = -T_r(\varphi_1) \tag{5}$$

$$I_L\ddot{\varphi_2} + c_0(\dot{\varphi_2} - \dot{\varphi_1}) + c_L\dot{\varphi_2} + k_0(\varphi_2 - \varphi_1) = T_m \tag{6}$$

As stated by Pesce *et al.* (2006), Lagrange's equations of motion cannot be applied directly to systems that have mass variation explicitly with the position. Even in simple cases, without considering the presence of none generalize force non-conservative, it is established equations of motion with excess or lack of terms in form $1/2(\partial m/\partial q)\dot{q}^2 2$, where $q$ is the generalized coordination. Therefore, the term $\frac{1}{2}\frac{dI_E(\varphi_1)}{d\varphi_1}\dot{\varphi_1}^2 2$ must be corrected by removing the constant $1/2$, so the correct equations of motion that describe the considered 2 DOF system with the additional harmonic excitation are:

$$I_E(\varphi_1)\ddot{\varphi_1} + \frac{dI_E(\varphi_1)}{d\varphi_1}\dot{\varphi_1}^2 + c_0(\dot{\varphi_1} - \dot{\varphi_2}) + c_E\dot{\varphi_1} + k_0(\varphi_1 - \varphi_2) = -T_r(\varphi_1) + T_0 cos(\omega t) \tag{7}$$

$$I_L\ddot{\varphi_2} + c_0(\dot{\varphi_2} - \dot{\varphi_1}) + c_L\dot{\varphi_2} + k_0(\varphi_2 - \varphi_1) = T_m. \tag{8}$$

### 2.2 Cylinder resistive and driving torques

According to Metallidis and Natsiavas (2003), the resistive torque $T_r(\varphi_1)$ is the result of force $F_p(\varphi_1)$ exerted by the compression of the gas mixture inside the cylinder. This force is given by:

$$F_p(\varphi_1) = pA_c \tag{9}$$

where $p$ is the pressure developed in the cylinder and $A_c$ is the cross-section area of the base of the cylinder. It is assumed that the gas mixture respects the polytropic law, therefore, the relationship between the pressure and volume is given by the equation:

$$pV^k = conste \tag{10}$$

where $V$ is the volume that the gas occupies in the cylinder and $k$ is the coefficient of adiabatic expansion with a value of 1.4 for air. The volume $V$ is determined as a function of $\varphi_1$, as follows:

$$V(\varphi_1) = V_c + [r + l - x_p(\varphi_1)]\frac{\pi D_p^2}{4} \tag{11}$$

where $V_c$ is the clearance volume and $D_p$ is the bore of the piston. Defining $K_x$ as the velocity coefficient that relates the velocity of the piston with the velocity of the generalized coordinate, $K_x = \dot{x}_p/\dot{\varphi_1}$, one obtains:

$$K_x = -r[sen(\varphi_1) + cos(\varphi_1)tg(\beta)]. \tag{12}$$

Therefore, the cylinder resistive torque is defined as:

$$\begin{aligned} &T_r(\varphi_1) = -K_x F_p(\varphi_1) \\ &T_r(\varphi_1) = r[sen(\varphi_1) + cos(\varphi_1)tg(\beta)](p - p_{atm})A_c. \end{aligned} \tag{13}$$

In this research the electric motor torque is modeled from a linearization of the torque-velocity curve, as discussed in Doughty (1988). Induction motors are known to have an almost linear relationship between torque and speed in the range close to synchronous speed. This characteristic allows its torque to be represented by a linear function. Thus, the torque delivered by the electric motor is modeled by:

$$T_m = C_0 + C_1\dot{\varphi_2} \tag{14}$$

where $C_0$ is the constant that intercepts the torque-velocity curve and $C_1$ is the slope of the torque-velocity curve.

### 2.3 Dimensionless equations of motion

To decrease integration time, dimensionless governing equations are used by introducing the dimensionless time $\tau = \omega_0 t$ with $\omega_0 = \sqrt{k_0(I_L + I_0)/I_L I_0}$, as defined by Metallidis and Natsiavas (2003), where $I_0$ is obtained by linearizing $I_E(\varphi_1)$.

$$I_0 = I_c + m_1 r^2 + \frac{1}{2}(m_2 + m_p)r^2 \tag{15}$$

The equations of motion in domain of $\tau$ are:

$$I_E(\varphi_1)\omega_0^2\varphi_1'' + \frac{dI_E(\varphi_1)}{d\varphi_1}\omega_0^2\varphi_1'^2 + c_0\omega_0(\varphi_1' - \varphi_2') + c_E\omega_0\varphi_1' + k_0(\varphi_1 - \varphi_2) = r[sen(\varphi_1) + cos(\varphi_1)tg(sen^{-1}(\lambda sen(\varphi_1)))](p - p_{atm})A_c + T_0 cos(\varphi_1'\tau) \tag{16}$$

$$I_L\omega_0^2\varphi_2'' + c_0\omega_0(\varphi_2' - \varphi_1') + c_L\omega_0\varphi_2' + k_0(\varphi_2 - \varphi_1) = C_0 + C_1\omega_0\varphi_2'. \tag{17}$$

## 3. RESULTS AND DISCUSSION

In this section, an analysis of the dynamic behavior of the system is carried out from numerical simulations by evaluating the influence of some parameters on torsional vibration. The integration method used in the simulations is the fourth-order Runge-Kutta.

### 3.1 Results without harmonic excitation

The equations of motion (16 and 17) are numerically integrated considering the dimensionless time $\tau$, with step $h = 0.01256637$ and using the initial conditions: $\varphi_1(0) = 0, \varphi_1'(0) = 0.5$ rad, $\varphi_2(0) = 0$ e $\varphi_2'(0) = 0$. To assess torsional vibration in the compressor shaft, the relative amplitude is defined as $\Delta\varphi = \varphi_1 - \varphi_2$. Critical operating situations are the cases that deserve more attention from the dynamic point of view. These situations are related to higher vibration amplitudes and occur in resonance regions, located near the natural frequencies. To determine these regions, system response was evaluated by varying the parameter $C_0$, as it leads to shaft rotation speed variation ($\varphi'_{1,med}$). Figure 3a shows the maximum amplitudes as a function of the average shaft rotation speed in the range from 0 to 4.41 rad, and Fig. 3b shows the maximum amplitude as a function of $C_0$, considering the region from 100 to 22000 N.m. In both cases, three distinct values of torsional stiffness, $k_0$, are used: $0.3 \times 10^6$, $0.3 \times 10^7$ and $0.3 \times 10^8$ N.m/rad.

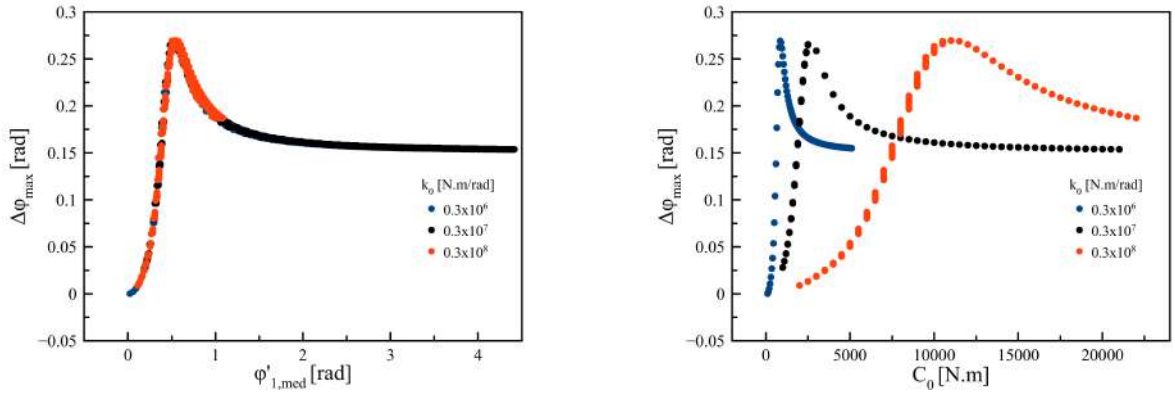


(a) (b)

Figure 3: Maximum amplitudes as a function of: a) average shaft rotation and b) $C_0$.

Figure 3a shows that the maximum amplitude occurs around $\varphi'_{1,med} = 0.54$ rad = 2492Hz, and has a value of 0.2746 rad for the three different cases of stiffness. Stiffness variation changes the natural frequency and, consequently, the resonance region. This change is not observed in Figure 3a because the system is dimensionless in time, and in this process, the parameter $\omega_0$ is used, which is also dependent on stiffness. However, considering dimensional values, the natural frequencies are different. Although the maximum amplitude is comprised in the same rotation speed range in

the three cases, the value of the constant $C_0$ is different for each situation. The values of $C_0$ associated with maximum amplitude response increases for higher stiffness values, as observed in Figure 3b.

A parametric analysis of the non-constant inertia is carried out and shows that the crank length ($r$) is the main parameter capable of increase nonlinearity in the inertia behavior, as showed the Figure 4. With the increase of crank length, there is a flattening at the peaks of the inertia response, this effect is more evident for $r$=150 mm.

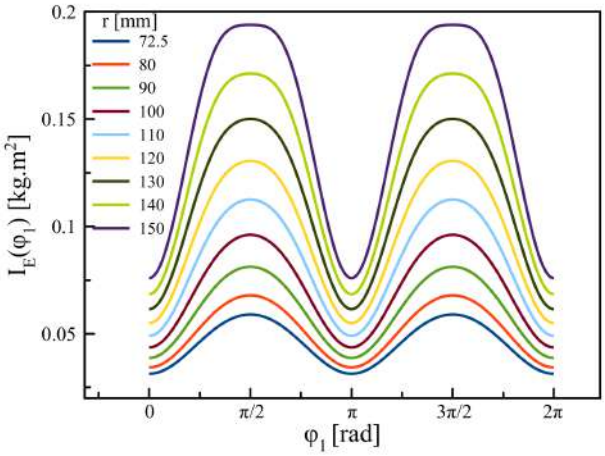


Figure 4: Effects of crank length on equivalent inertia $I_E(\varphi_1)$.

In order to evaluate how the crank length variation influences the dynamical response, Figure 5 presents steady-state response in phase spaces for different values of $r$. We observe that the torsional vibration amplitude increases as the crank length increases, as well as the phase space changes its shape. Although the system presents periodic behavior, the influence of nonlinearity is evident in the phase of spaces, which is deformed.

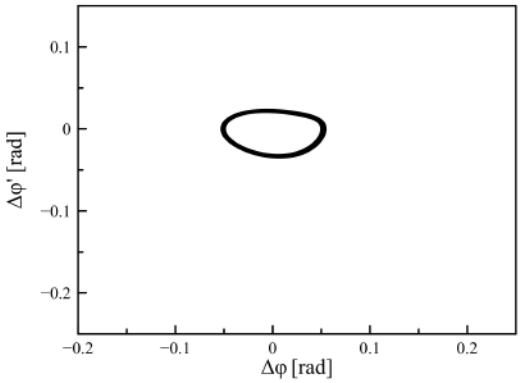


(a) $r = 72.5$ mm

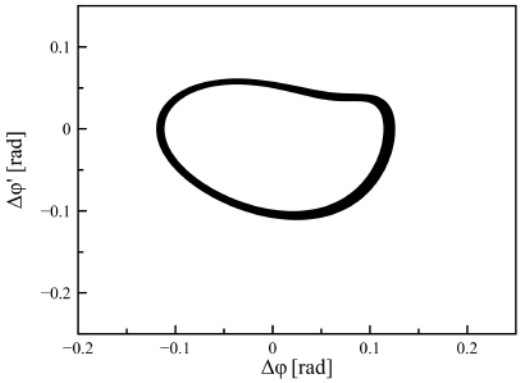


(b) $r = 110$ mm

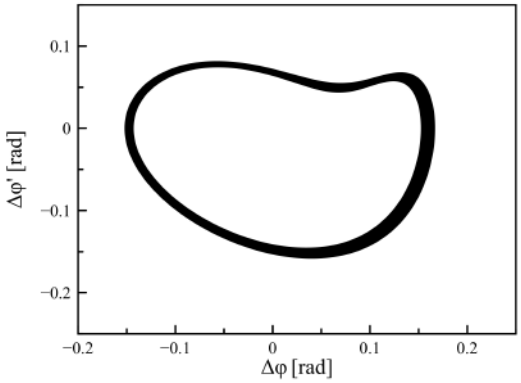


(c) $r = 130$ mm

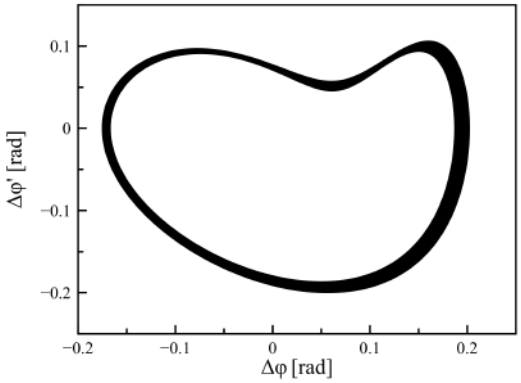


(d) $r = 150$ mm

Figure 5: Phase spaces for different values of crank length.

Figure 6 presents an analysis of the system response in frequency domain for each values of crank length ($r$) evaluated. The frequency spectrum shows that the response is composed of frequencies that are multiples of the rotating frequency for each case. The variable inertia $I_E(\varphi_1)$ acts as an unbalance to the shaft, causing torsional vibrations. Thus, it is coherent that rotation frequency appears in the frequency response. The presence of nonlinearities results in the appearance of more frequency components, as showed in Figure 6 . Note that the highest values of crank length, $r = 150$ mm, presents more components in frequency, being related to the deformations in phase space observed in Figure 5. If an equivalent linear model with constant inertia was assumed, there would have no torsional vibration in steady state regime as the vibration occurs due to the non-constant inertia.

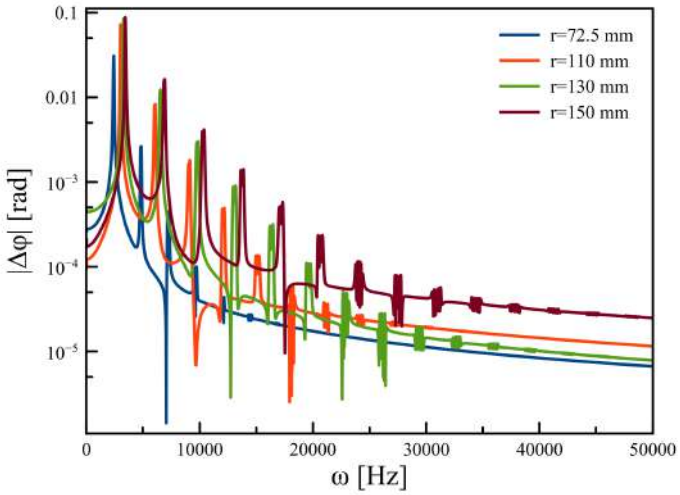


Figure 6: Harmonics with the variation of the crank length.

### 3.2 Results with harmonic excitation

In this section, an additional torsional harmonic excitation is considered in order to evaluate situations associated with higher responses amplitudes. The excitation frequency is considered to be equal to the shaft rotation frequency. Two distinct values of stiffness are considered, $k_0 = 0.3{\times}10^7$ and $k_0 = 0.3{\times}10^6$ N.m/rad, at critical operating condition, which are associated with $C_0 = 2500$ and $C_0 = 2500\ 850$ N.m, respectively. All results of this section were obtained from the numerical integration with time step $h = 0.00418879$ and with the same initial conditions used in the previous simulations ($\varphi_1(0) = 0, \varphi_1'(0) = 0.5$ rad, $\varphi_2(0) = 0$ e $\varphi_2'(0) = 0$). Figure 7 presents phase space in steady state regime together with the Poincaré section for the first set of analyzed situations, with $C_0 = 2500$ N.m, torsional stiffness of $k_0$ = $0.3{\times}10^7$ N.m/rad and for different forcing amplitudes.

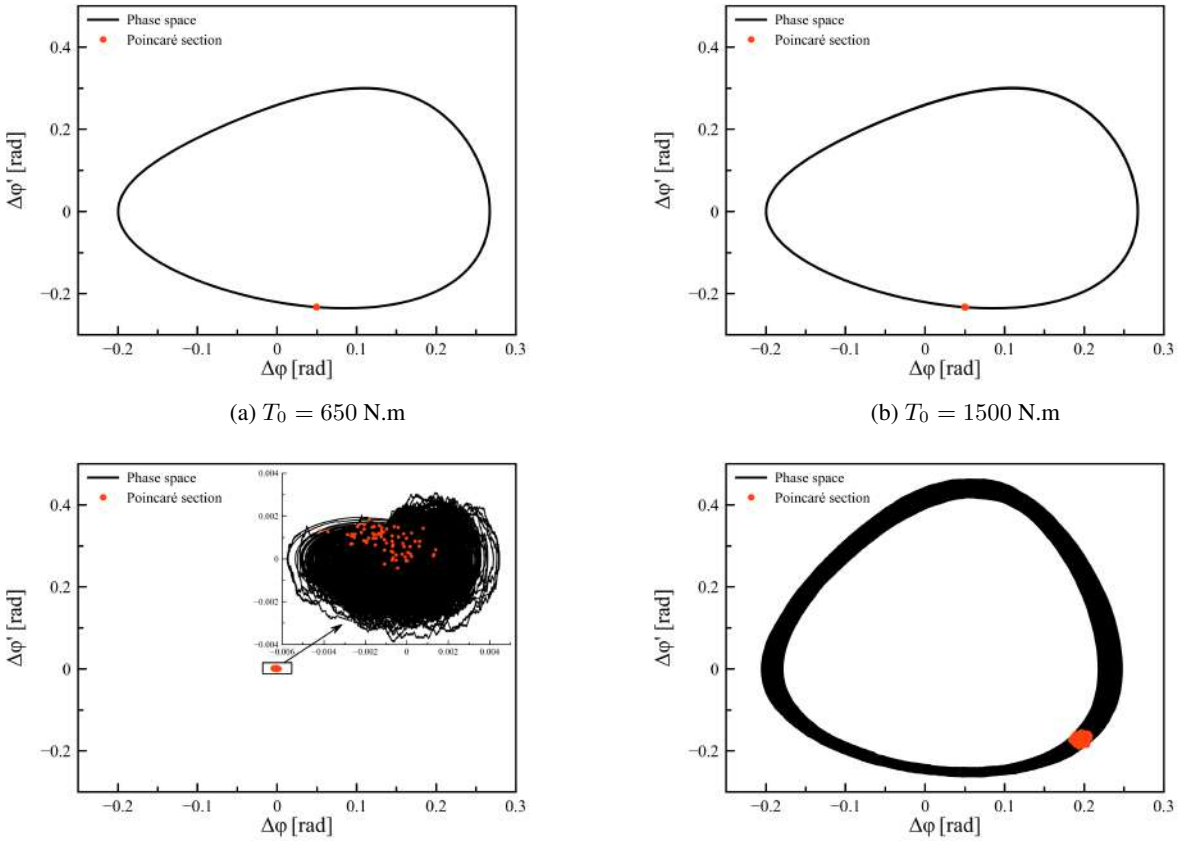


(a) $T_0 = 650$ N.m

(b) $T_0 = 1500$ N.m

(c) $T_0 = 60000$ N.m

(d) $T_0 = 650000$ N.m

Figure 7: Phase space and Poincaré section for $C_0 = 2500$ N.m, $k_0 = 0.3{\times}10^7$ N.m/rad and different values of $T_0$.

The responses presented by the system with torque amplitude up to 1500 N.m (Figures 7a and 7b) are periodic. However, when $T_0$ is increased to 60000 and 650000 N.m (Figures 7c and 7d), more complex responses are observed. In addition, the more complex behavior, Figure 7c, causes a significant decrease in the maximum response amplitudes.

To have a global view of system dynamical behavior, a bifurcation diagram is constructed by increasing the torque amplitude, $T_0$, and showing the relative angular displacement, $\Delta\varphi$, as presented in Figure 8. The same initial condition for each excitation amplitude is considered and the first 9000 points is disregarded, considered as transient. From Figure 8, we observe that there are periodic regions (0 to $1.2{\times}10^5$ N.m) and more complex regions ($1.2{\times}10^5$ to $10^6$ N.m) that can be associated with chaotic motion.

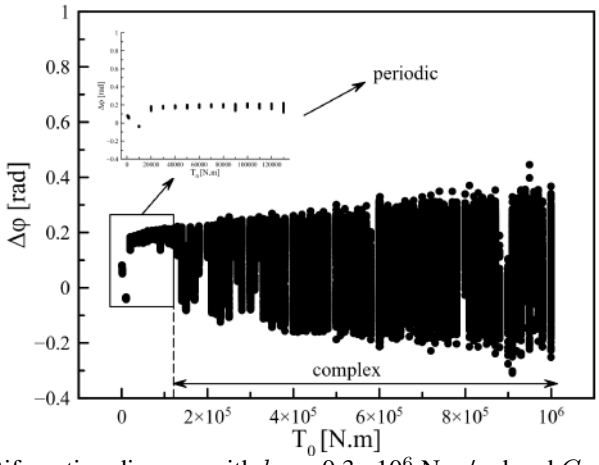


Figure 8: Bifurcation diagram with $k_0 = 0.3{\times}10^6$ N.m/rad and $C_0 = 850$ N.m.

Figure 9 presents phase space in steady state regime, together with the Poincaré section, for $C_0 = 850$ N.m, torsional

stiffness of $k_0 = 0.3\times10^6$ N.m/rad and different forcing amplitudes.

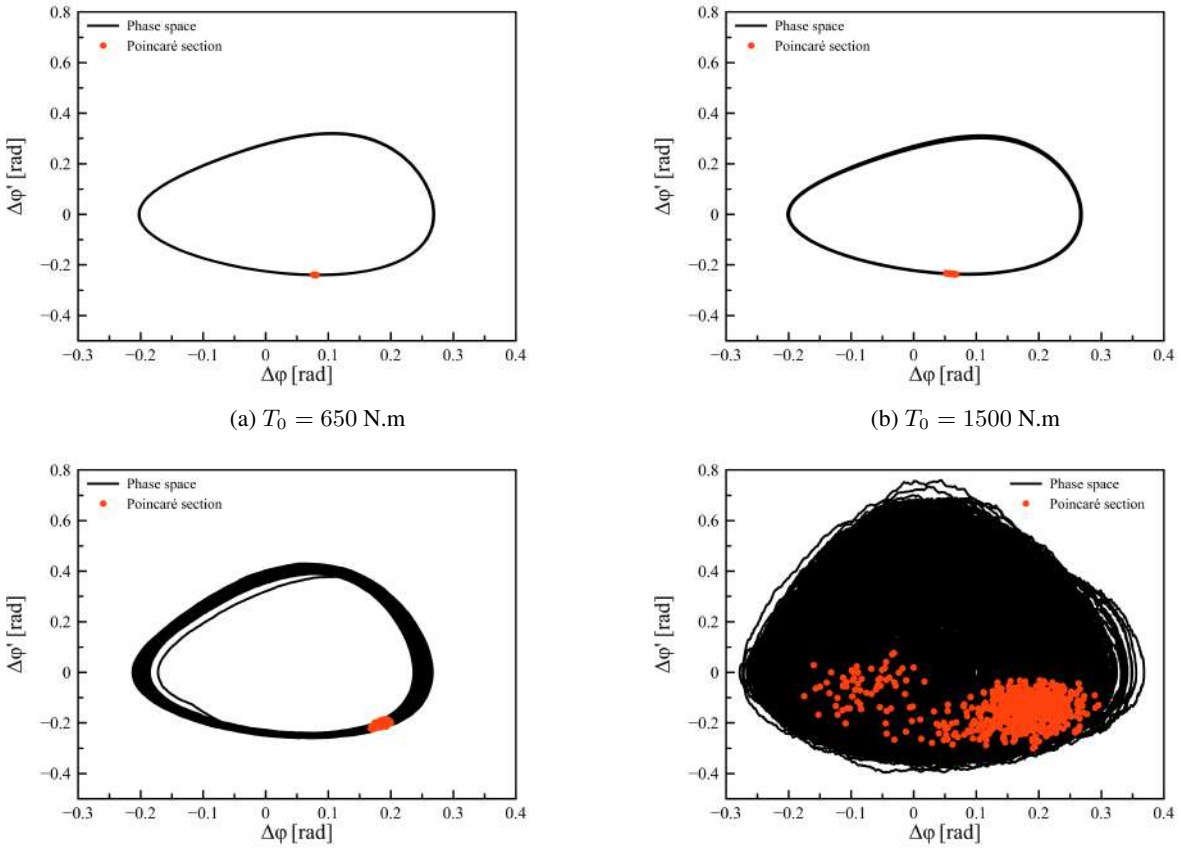


(a) $T_0 = 650$ N.m

(b) $T_0 = 1500$ N.m

(c) $T_0 = 60000$ N.m

(d) $T_0 = 650000$ N.m

Figure 9: Phase space and Poincaré section for $C_0 = 850$ N.m, $k_0 = 0.3\times10^6$ N.m/rad and different values of $T_0$.

Figures 9a and 9b shows that for the harmonic torque amplitudes of 650 and 1500 N.m, system presents periodic responses, as occurred in the previous analyzed cases with $k_0 = 0.3\times10^7$ N.m/rad. With $T_0 = 60000$ N.m (Figure 9c), a non-periodic behavior starts to develop, and with 650000 N.m (Figure 9d), a complex behavior with high amplitudes is observed, that can be associated with a chaotic motion. Thus, it is noteworthy that the decrease in the stiffness can induce the compressor shaft to develop more complex behaviors.

## 4. CONCLUSIONS

In this work, a simplified nonlinear model of a single cylinder reciprocating compressor attached to an electric motor through a shaft is of concern. The nonlinearity arises from a variable inertia of rod-crank-piston mechanism. Although there are similar models in the literature, the investigated dynamical model is unique and the mathematical modelling is addressed in the paper. At first, steady-state torsional vibration of compressor shaft was evaluated for different geometric parameters and in different operating conditions. The influence of the nonlinearity was evident in system response. It was observed that the increase of the nonlinearity, due to higher values of crank length, lead to more deformed phase spaces, resulting in the presence of more frequency components in the response. In the sequence, an additional torsional harmonic excitation was considered, in order to evaluate situations associated with higher responses amplitudes. In this analysis, system presented a more rich dynamics, and periodic and complex non-periodic behaviors were observed. Thus, results showed the importance of considering nonlinearities due to the variable inertia of the mechanism in the torsional vibration analysis, specially when considering geometric parameters associated with higher nonlinearities.

## 5. ACKNOWLEDGMENTS

The authors would like to acknowledge the support of the Brazilian Research Agencies FAPEMA, CAPES and CNPq (grants 310850/2019-3 and 433730/2018-8) for the support to this research work.

## 6. REFERENCES

Brusa, E., Delprete, C. and Genta, G., 1997. "Torsional vibration of crankshafts: Effects of non-constant moments of inertia". *Journal of Sound and Vibration*, Vol. 205, No. 2, pp. 135–150. ISSN 0022460X. doi:10.1006/jsvi.1997.0964.

Doughty, S., 1988. *Mechanics of machines*. John Wiley a. Sons, New York.

Huang, Y., Yang, S., Zhang, F., Zhao, C., Ling, Q. and Wang, H., 2012. "Non-linear torsional vibration characteristics of an internal combustion engine crankshaft assembly". *Chinese Journal of Mechanical Engineering (English Edition)*, Vol. 25, No. 4, pp. 797–808. ISSN 10009345. doi:10.3901/CJME.2012.04.797.

Metallidis, P. and Natsiavas, S., 2003. "Linear and nonlinear dynamics of reciprocating engines". *International Journal of Non-Linear Mechanics*, Vol. 38, No. 5, pp. 723–738.

Pasricha, M.S. and Carnegie, W.D., 1976. "EFFECTS OF VARIABLE TORSIONAL VIBRATIONS INERTIA ON THE DAMPED OF DIESEL ENGINE SYSTEMS". *Journal of Sound and Vibration*, Vol. 46, No. 3, pp. 339–345.

Pasricha, M.S. and Carnegie, W.D., 1979. "Formulation of the equations of dynamic motion including the effects of variable inertia on the torsional vibrations in reciprocating engines, part I". *Journal of Sound and Vibration*, Vol. 66, No. 2, pp. 181–186. ISSN 10958568. doi:10.1016/0022-460X(79)90664-3.

Pesce, C.P., Tannuri, E.A. and Casetta, L., 2006. "The Lagrange Equations for Systems with Mass Varying Explicitly with Position: Some Applications to Offshore Engineering". *Journal of the Brazilian Society of Mechanical Sciences and Engineering*, Vol. 28, No. 4, pp. 496–504. ISSN 18063691. doi:10.1590/S1678-58782006000400015.

Wachel, J.C. and Szenasi, F.R., 1993. "Analysis of torsional vibrations in rotating machinery". *Proceedings of the twenty-second Turbomachinery Symposium*, pp. 127–151.

Wachel, J., Tison, J. *et al.*, 1994. "Vibrations in reciprocating machinery and piping systems." In *Proceedings of the 23rd Turbomachinery Symposium*. Texas A&M University. Turbomachinery Laboratories.

## 7. RESPONSIBILITY NOTICE

The authors, Nícolas da Silva Dias and Aline Souza de Paula, are solely responsible for the printed material included in this paper.